◀ **Fig. 3** HAT activity of MOZ is required for transformation activity by MOZ–TIF2. **a** Structure of MOZ–TIF2 and its point mutants, Q654E/G657E and G654E. **b** HAT activity of WT and point mutants of MOZ. WT, G654E, Q654E/G657E MOZ or empty vector were cotransfected into 293FT cells. Immunoprecipitates were collected and cultured with histone H2A/B, H3, H4 and C^{14} labeled-acetyl-coenzyme A. C^{14} labeled acetylated histone was detected by BAS. Although HAT activity was reduced in both point mutants of MOZ compared to WT MOZ, G657E MOZ retained subtle HAT activity. Data are mean ± SD ($n = 3$). **c** Colony numbers of cells transduced with WT, G654E, Q654E/G657E MOZ–TIF2 or empty vector. WT and G657E MOZ–TIF2 showed transformation activity, which was not observed in cells transduced with Q654E/G657E MOZ–TIF2 or empty vector. **d** First round and 4th round colonies of cells transduced with WT, G654E, Q654E/G657E MOZ–TIF2 or empty vector were collected and analyzed for expression levels of *Hoxa9, Hoxa10* by qRT-PCR analysis. Expression level of *Hoxa10* was significantly lower in colony cells transduced with both mutants compared to WT MOZ–TIF2 at 1st round, but reached to the similar levels at 4th round in cells with Q654E/G657E MOZ–TIF2. Data are mean ± SD ($n = 3$). $^{**}P < .01$. **e** Kaplan–Meier survival curve analysis of mice transplanted with WT, G657E or Q654E/G657E MOZ–TIF2. All of the mice transplanted with WT MOZ–TIF2 and 7 out of 10 mice transplanted with G657E MOZ–TIF2 developed AML, while none of the mice transplanted with Q654E/G657E MOZ–TIF2 developed leukemia. **f** FLAG-tagged WT, G654E, Q654E/G657E MOZ–TIF2 or empty vector were cotransfected into 293FT cells together with HA-tagged Brpf1. Immunoprecipitates with anti-FLAG antibody (M2 IP) or cell lysates (Extracts) were subjected to immunoblotting with anti-HA or anti-FLAG antibodies. WT and both point mutants of MOZ–TIF2 were able to interact with Brpf1

domain [18]. Thus, we firstly constructed deletion mutant of BRPF1 (Δ1–222) which lacks interacting domain with MOZ, and performed immunoprecipitation assay. This mutant BRPF1 consistently lacked potential to form complex with MOZ (Fig. 1a). Using wild-type (WT) and deletion mutant of BRPF1, we next examined the effect of *Brpf1* knockdown in MOZ–TIF2 leukemic cells. MOZ–TIF2-tranduced mouse BM cells were subsequently transduced with Brpf1 shRNA by lentivirus system. Knockdown efficiencies were confirmed by qRT-PCR and western blotting (Fig. 1b, c). *Brpf1* knockdown resulted in marked decrease of colony numbers, which was rescued by WT human BRPF1 but not by mutant human BRPF1 (Fig. 1d). We further examined the effect of *Brpf1* knockdown on transcriptional activation induced by MOZ–TIF2. As expected, *Brpf1* knockdown led to decrease of *Hoxa9*, *Hoxa10* and *Meis1* expression (Fig. 1E). This decrease was again restored by WT human BRPF1 but not by mutant human BRPF1. These data suggest that Brpf1 contributes to *Hoxa9*, *Hoxa10* and *Meis1* transcription, which are overexpressed in AML patients with MOZ fusions [15].

Interacting domain of MOZ with Brpf1 is essential for initiation of MOZ–TIF2 leukemia

To investigate the importance of MOZ interaction with Brpf1, we firstly constructed several MOZ–TIF2 mutants as shown in Fig. 2a, and performed immunoprecipitation assay. The 760–783 region of MOZ was previously reported to be the interacting domain with BRPF1 [18]. However, deletion of the region 760–783 did not affect interaction of MOZ–TIF2 with BRPF1 in our condition (Fig. 2b). We previously found that the 760–783 region is required for histone acetyltransferase (HAT) activity [1]. Deletion analysis showed that there is another interacting domain that localized at HAT domain (N488–664) (Fig. 2c). For the following assay, we selected two deletion mutants of MOZ–TIF2, previously reported mutant Δ760–783, and Δ311–664 which lacks the novel interacting domain. We transduced these two deletion mutants, WT MOZ–TIF2 or empty vector to BM progenitors and performed colony formation assay. While WT MOZ–TIF2 cells were capable of forming colonies for several times of replating, others including two deletion mutants of MOZ–TIF2 lost their ability to form colonies in the 2nd round (Fig. 2d). 1st round colony cells were collected and analyzed for expression levels of *Hoxa9*, *Hoxa10* and *Meis1* by qRT-PCR. Corresponding to the results of colony formation assay, transcriptional activation of *Hoxa9* and *Hoxa10* induced by WT MOZ–TIF2 was not observed by two deletion mutants (Fig. 2f). Furthermore, none of the mice injected with BM cells transduced with either of the deletion mutants of MOZ–TIF2 developed AML (Fig. 2e).

HAT activity of MOZ contributes to leukemic transformation induced by MOZ–TIF2

The 760–783 and 488–664 regions were localized in MOZ HAT domain [1]. Although HAT activity is reported to be dispensable for leukemogenesis by MOZ–TIF2 [10], we evaluated the possible association between lack of MOZ HAT activity and loss of leukemogenic potential in Δ311–664 or Δ760–783 mutant MOZ–TIF2. MOZ is the founding member of the MYST family of HATs, which share the conserved MYST domains [5]. To assess the importance of MOZ HAT activity, we constructed previously reported MOZ HAT-deficient G657E mutant as well as Q654E/G657E mutant according to the HAT-deficient mutant of TIP60 (Fig. 3a) [8, 19, 20]. Firstly, we assessed HAT activity of these two HAT-deficient mutants using immunoprecipitates with anti-FLAG antibody, obtained from 293FT cells transfected with FLAG-tagged WT or mutant MOZ (Fig. 3b). WT MOZ showed HAT activity for Histones H2A, H3, H4. Although both HAT-deficient mutants G657E and Q654E/G657E possessed markedly low HAT activity compared to WT MOZ, HAT activity slightly remained in G657E mutant. Next, we examined the colony formation activity of these two HAT-deficient mutants. BM progenitors were transduced with WT, G657E, Q654E/G657E mutant of MOZ–TIF2 or empty vector and subsequently cultured in methylcellulose media. Through 4 rounds of replating, WT and G657E mutant, but not Q654E/G657E mutant, were capable of

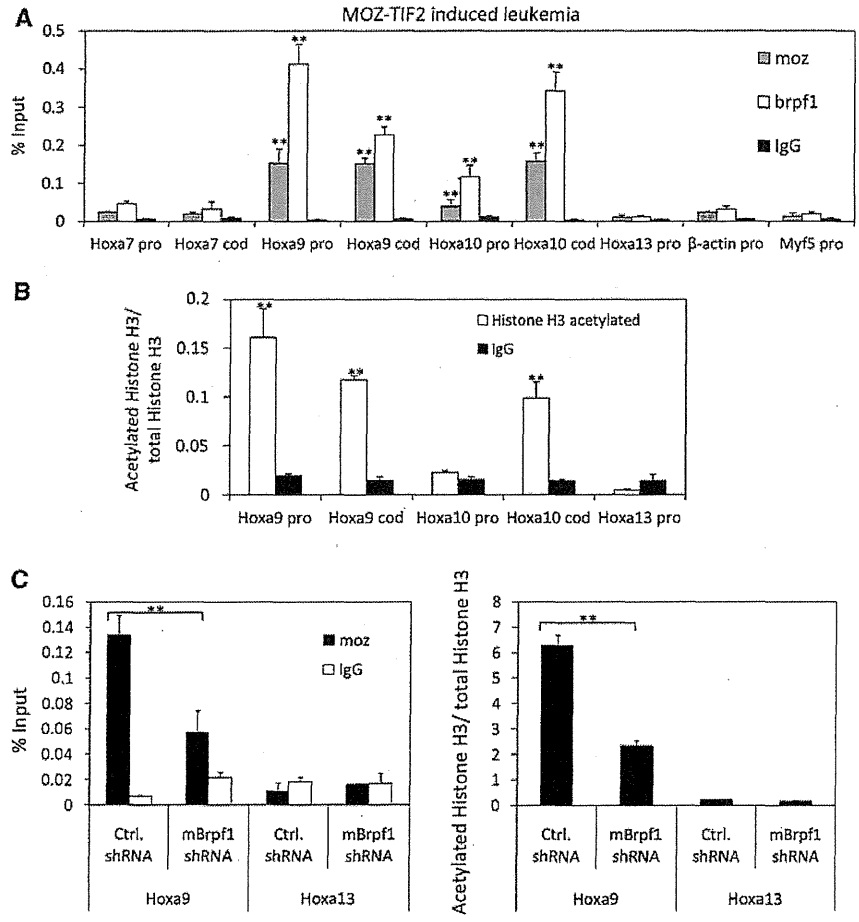

Fig. 4 *Hoxa9* and *Hoxa10* are direct targets of Moz and Brpf1. **a, b** Relative binding of Moz, Brpf1 and acetylated Histone H3 to the promoter and coding region of indicated genes in MOZ–TIF2 leukemic cells. Moz and Brpf1 colocalized at *Hoxa9* and *Hoxa10* genes, in which acetylated Histone H3 levels were higher compared to other tested genes. Data are mean ± SD ($n = 3$). $^{**}P < .01$. **c** Relative binding of Moz and acetylated Histone H3 to the promoter region of *Hoxa9* and *Hoxa13* after *Brpf1* knockdown. Downregulation of Brpf1 reduced the localization of Moz on promoter region of Hoxa9 and also reduced Histone H3 acetylation. Data are mean ± SD ($n = 3$). $^{**}P < .01$

inducing serial replating activity (Fig. 3c). *Hoxa10* expression levels of the 1st round colony cells were decreased by both mutants, but increased to similar level as WT in the 4th round by G657E mutant (Fig. 3d). BM progenitors transduced with WT, G657E or Q654E/G657E mutant of MOZ–TIF2 were also transplanted into sublethally irradiated recipient mice. G657E mutant MOZ–TIF2 led to development of AML in a subset of mice as reported before [8]. However, Q654E/G657E mutant MOZ–TIF2 showed no potential to initiate leukemia (Fig. 3e). These two HAT-deficient mutants were confirmed to be capable of interacting with Brpf1 at similar level as WT MOZ–TIF2 (Fig. 3f). These results indicate that even in a slight level, MOZ HAT activity is required for leukemogenic activity induced by MOZ–TIF2, which was independent of interaction with Brpf1.

Hoxa9 and *Hoxa10* are direct targets of MOZ and BRPF1 complex

To understand the mechanism of leukemic transformation induced by MOZ–TIF2, we performed chromatin immunoprecipitation (ChIP) assay using MOZ–TIF2 colony cells. As shown in Fig. 4a, MOZ and Brpf1 colocalized on chromatin within *Hoxa9* and *Hoxa10* locus, suggesting that these genes are direct targets of MOZ and Brpf1 complex. Indeed, Histone H3 acetylation level was upregulated at target *Hoxa9* and *Hoxa10* genes (Fig. 4b). We also performed ChIP assay using Brpf1 shRNA expressing MOZ–TIF2 colony cells. Depletion of Brpf1 resulted in reduction of MOZ localization on target *Hoxa9* gene, suggesting that Brpf1 enhances the enrichment level of MOZ localization on target genes (Fig. 4c). Together, these data suggest that Brpf1 leads to MOZ localization on the target genes, *Hoxa9* and *Hoxa10*, which enhance histone H3 acetylation and transcriptional activation of these genes, eventually resulting in development of AML.

Hoxa9 overexpression is not substantial for transformation of MOZ–TIF2 in Brpf1 downregulated cells

Previously, HOXA9 alone was reported to be sufficient for leukemic transformation in vitro [11, 13]. Because MOZ–

TIF2 leukemic cells exhibited lower expression level of *Hoxa9*, we assessed the effect of HOXA9 overexpression in MOZ–TIF2 leukemic cells with *Brpf1* knockdown. Unexpectedly, enforced expression of human HOXA9 failed to restore colony formation ability that was impaired by *Brpf1* knockdown (Fig. 5a, b). Downregulation of endogenous *Hoxa9*, *Hoxa10* and *Meis1* by depletion of Brpf1 was not restored by HOXA9 overexpression (Fig. 5c), suggesting again that Brpf1 contributes to transcriptional activation of not only *Hoxa9* but also *Hoxa10* and *Meis1*, both of which do influence the leukemic transformation activity. [12, 14, 21, 22].

Discussion

HOX genes are deregulated in a subset of AML patients, which strongly correlate with poor prognosis [23, 24]. Human AML with MOZ fusions applies to this subset of group, with high levels of *HOXA9* and *HOXA10* [15]. Herein, upregulation of *HOX* genes may contribute to the leukemogenesis in MOZ-related AML. To assess the mechanism and the role of *HOX* genes deregulation in MOZ-related leukemias, we focused on Brpf1. Brpf1, a component of MOZ complex, possesses PHD finger domain, bromodomain and PWWP domain [16, 17, 25]. PWWP domain and bromodomain of Brpf1 directly bind to Histones and are required for chromatin targeting by Brpf1 [16]. Previous study in zebrafish and medaka suggested that Brpf1 is required for the maintenance of *Hox* genes expression through Moz-dependent histone acetylation. [16, 17] Thus, Brpf1 may contribute to upregulation of *HOX* genes in MOZ-related leukemias.

In this study, we have demonstrated that Brpf1 plays an important role in leukemogenesis induced by MOZ–TIF2. Our data indicated that *Hoxa9* and *Hoxa10* were direct

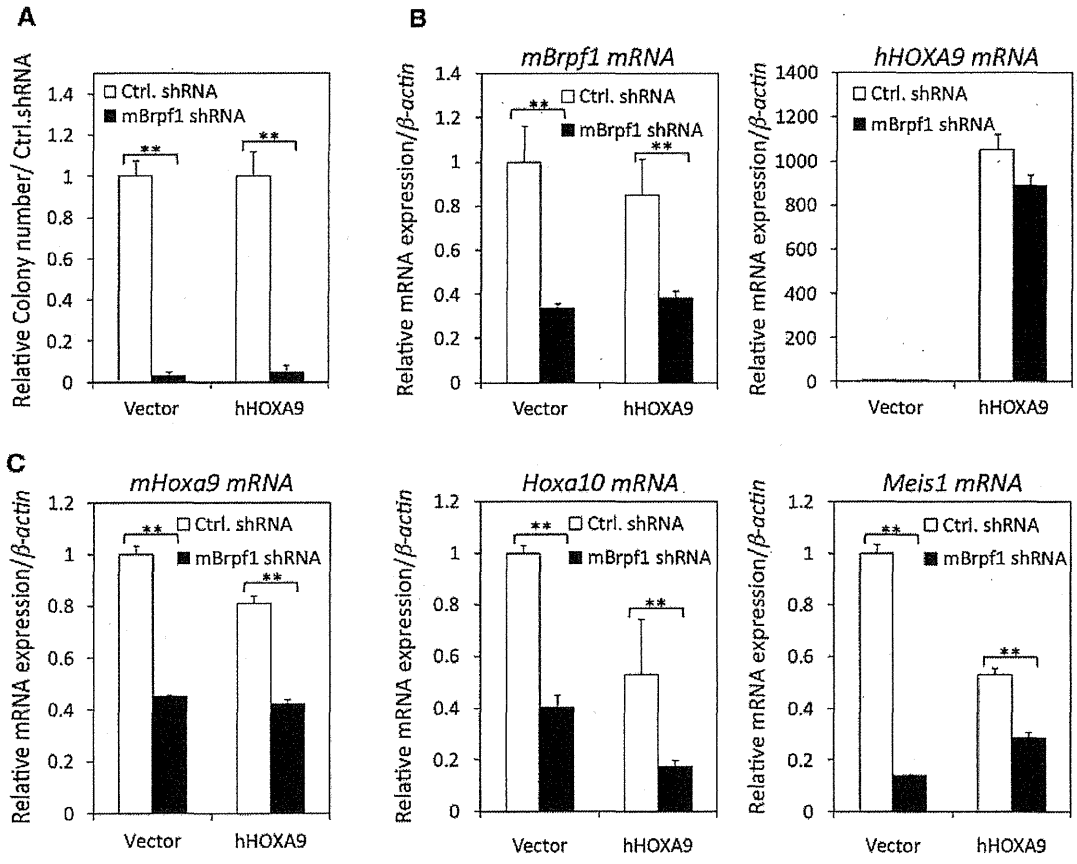

Fig. 5 Effect of HOXA9 overexpression on MOZ–TIF2 leukemic cells with downregulated Brpf1. **a** Relative colony number of MOZ–TIF2 leukemic cells transduced with control shRNA or Brpf1 shRNA. Overexpression of wild-type HOXA9 was not sufficient to restore colony formation activity of MOZ–TIF2 leukemic cells with downregulated Brpf1. Data are mean ± SD ($n = 3$). $^{**}P < .01$. **b** Expression of murine *Brpf1* and human *HOXA9* after Brpf1 shRNA and HOXA9 overexpression. **c** Effects of Brpf1 shRNA and HOXA9 overexpression on expression levels of *Hoxa9*, *Hoxa10* and *Meis1* in Brpf1 downregulated MOZ–TIF2 leukemic cells. Reduced expressions of *Hoxa9*, *Hoxa10* and *Meis1* by *Brpf1* knockdown were sustained in cells with HOXA9 overexpression. Data are mean ± SD ($n = 3$). $^{**}P < .01$

targets of MOZ and BRPF1 in MOZ–TIF2 leukemic cells. Because depletion of Brpf1 exhibited decreased level of MOZ localization on these target genes, resulting in loss of transformation ability induced by MOZ–TIF2, we suggest that Brpf1 promotes MOZ to localize on chromatin of these target genes. Brpf1 recruits MOZ to the target genes and upregulates transcriptional activation through histone H3 acetylation. Since binding of MOZ–TIF2 to the *Meis1* gene locus is weak compared to its binding to *Hoxa9* and *Hoxa10* (data not shown), MOZ–TIF2 is unlikely to regulate the expression of Meis1 directly. Our data also indicate that HAT activity of MOZ is essential for transformation activity induced by MOZ–TIF2. HAT-deficient MOZ–TIF2 was incapable of not only deregulating *Hox* genes, but also initiating leukemia. We suggest that MOZ or MOZ-fusion/BRPF1 complex upregulates *HOX* genes mediated by MOZ-dependent histone acetylation, which finally leads to the development of leukemia.

Although HOXA9 alone possesses transformation activity, enforced expression of human HOXA9 unexpectedly failed to rescue transformation activity abolished by Brpf1 depletion. There are two possible reasons to be considered. Firstly, *Hoxa10* and *Meis1*, both of which were downregulated in Brpf1 depleted cells remained in lower level compared to control cells despite HOXA9 overexpression. This may suggest that downregulation of several *HOX* genes other than *HOXA9* may result in loss of leukemic transformation. Secondly, Brpf1 may be required for HOXA9 function and its downstream pathway. Further study is required to determine the association of Brpf1 and Hoxa9 in the maintenance of transformation activity in AML cells.

Previously, we have shown that upregulation of M-CSFR is critical for the regulation of AML stem cells in MOZ–TIF2 leukemia, and STAT5, which was highly phosphorylated in M-CSFR high cells but not in low cells, may contribute to the clonal expansion and stem cell maintenance [2]. In this study, we demonstrated that deletion mutant of MOZ–TIF2 lacking interacting domain with Brpf1 lost its transformation activity. However, M-CSFR upregulation was maintained in BM cells transduced with this mutant MOZ–TIF2. Furthermore, Hoxa9 expression was upregulated in both M-CSFR-high cells and low cells [2]. Therefore, MOZ/BRPF1/HOX pathway should be considered as independent of PU.1/M-CSFR pathway (Fig. 6). Collectively, our study reveals that MOZ/BRPF1/HOX pathway plays a crucial role in the development of leukemia induced by MOZ–TIF2. For efficient induction of AML, block in the normal hematopoietic differentiation program together with unrestrained growth is required. Several AML-associated chromosomal translocations require additional mutations for the progenitors to gain both of these functions [26, 27]. However, in terms of MOZ–TIF2 leukemia, although increased expression of *HOX* genes may be insufficient to induce AML in a short period, increased phosphorylation of STAT5 mediated by PU.1/M-CSFR pathway would accelerate the development of leukemia. Thus, both MOZ/BRPF1/HOX pathway and PU.1/M-CSFR pathway are essential for the development of MOZ–TIF2 AML.

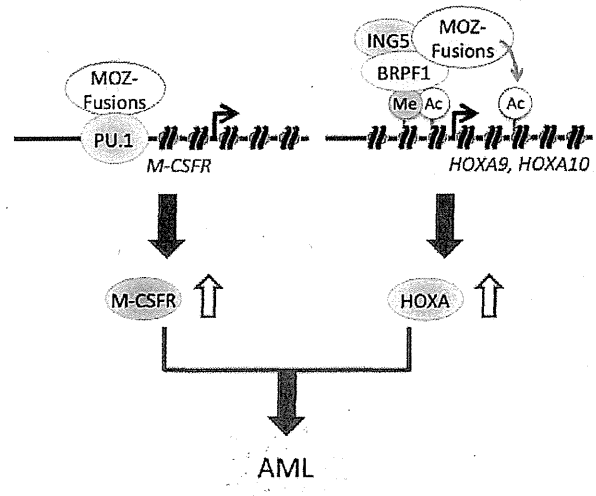

Fig. 6 Model of leukemogenic mechanism induced by MOZ–TIF2. Apart from PU.1/M-CSFR pathway, BRPF1/HOX pathway is essential for leukemogenesis by MOZ–TIF2. BRPF1 enhances the localization of MOZ on target genes such as *HOXA9* or *HOXA10*, and promotes Histone H3 acetylation, which may result in transcriptional upregulation of target genes, finally contributing to the development of leukemia

Acknowledgments This work was supported in part by Grants-in-Aid from the Ministry of Health, Labor, and Welfare; the Ministry of Education, Culture, Sports, Science, and Technology; and National Cancer Center Research and Development Fund.

Conflict of interest The authors declare no competing financial interests.

References

1. Kitabayashi I, Aikawa Y, Nguyen LA, et al. Activation of AML1-mediated transcription by MOZ and inhibition by the MOZ–CBP fusion protein. EMBO J. 2001;20(24):7184–96.
2. Aikawa Y, Katsumoto T, Zhang P, et al. PU.1-mediated upregulation of CSF1R is crucial for leukemia stem cell potential induced by MOZ–TIF2. Nat Med. 2010;16(5):580–5.
3. Rokudai S, Aikawa Y, Tagata Y, et al. Monocytic leukemia zinc finger (MOZ) interacts with p53 to induce p21 expression and cell-cycle arrest. J Biol Chem. 2009;284(1):237–44.
4. Katsumoto T, Aikawa Y, Iwama A, et al. MOZ is essential for maintenance of hematopoietic stem cells. Genes Dev. 2006;20(10):1321–30.
5. Borrow J, Stanton VP Jr, Andresen JM, et al. The translocation t(8;16)(p11;p13) of acute myeloid leukaemia fuses a putative

acetyltransferase to the CREB-binding protein. Nat Genet. 1996;14:33–41.
6. Kitabayashi I, Aikawa Y, Yokoyama A, et al. Fusion of MOZ and p300 histone acetyltransferases in acute monocytic leukemia with a t(8;22)(p11;q13) chromosome translocation. Leukemia. 2001;15:89–94.
7. Chaffanet M, Gressin L, Preudhomme C, et al. MOZ is fused to p300 in an acute monocytic leukemia with t(8;22). Genes Chromosomes Cancer. 2000;28:138–44.
8. Deguchi K, Ayton PM, Carapeti M, et al. MOZ–TIF2-induced acute myeloid leukemia requires the MOZ nucleosome binding motif and TIF2-mediated recruitment of CBP. Cancer Cell. 2003;3:259–71.
9. Yang XJ, Ullah M. MOZ and MORF, two large MYSTic HATs in normal and cancer stem cells. Oncogene. 2007;26:5408–19.
10. Carapeti M, Aguiar RC, Goldman JM, et al. A novel fusion between MOZ and the nuclear receptor coactivator TIF2 in acute myeloid leukemia. Blood. 1998;91:3127–33.
11. Calvo KR, Sykes DB, Pasillas M, Kamps MP. Hoxa9 immortalizes a granulocyte macrophage colony stimulating factor dependent promyelocyte capable of biphenotypic differentiation to neutrophils or macrophages independent of enforced Meis expression. Mol Cell Biol. 2000;20:3274–85.
12. Buske C, Feuring-Buske M, Antonchuk J, et al. Overexpression of HOXA10 perturbs human lymphomyelopoiesis in vitro and in vivo. Blood. 2001;97:2286–92.
13. Thorsteinsdottir U, Mamo A, Kroon E, et al. Overexpression of the myeloid leukemia associated Hoxa9 gene in bone marrow cells induces stem cell expansion. Blood. 2002;99:121–9.
14. Thorsteinsdottir U, Sauvageau G, Hough MR, et al. Overexpression of HOXA10 in murine hematopoietic cells perturbs both myeloid and lymphoid differentiation and leads to acute myeloid leukemia. Mol Cell Biol. 1997;17:495–505.
15. Camós M, Esteve J, Jares P, et al. Gene expression profiling of acute myeloid leukemia with translocation t(8;16)(p11;p13) and MYST3-CREBBP rearrangement reveals a distinctive signature with a specific pattern of HOX gene expression. Cancer Res. 2006;66(14):6947–54.
16. Hibiya K, Katsumoto T, Kondo T, et al. Brpf1, a subunit of the MOZ histone acetyl transferase complex, maintains expression of anterior and posterior Hox genes for proper patterning of craniofacial and caudal skeletons. Dev Biol. 2009;329(2):176–90.
17. Laue K, Daujat S, Crump JG, et al. The multidomain protein Brpf1 binds histones and is required for Hox gene expression and segmental identity. Development. 2008;135:1935–46.
18. Ullah M, Pelletier N, Xiao L, et al. Molecular architecture of quartet MOZ/MORF histone acetyltransferase complexes. Mol Cell Biol. 2008;28(22):6828–43.
19. Ikura T, Ogryzko VV, Grigoriev M, et al. Involvement of the TIP60 histone acetylase complex in DNA repair and apoptosis. Cell. 2000;102(4):463–73.
20. Perez-Campo FM, Borrow J, Kouskoff V, Lacaud G. The histone acetyl transferase activity of monocytic leukemia zinc finger is critical for the proliferation of hematopoietic precursors. Blood. 2009;113(20):4866–74.
21. Thorsteinsdottir U, Kroon E, Jerome L, et al. Defining roles of Hox and MEIS1 genes in induction of acute myeloid leukemia. Mol Cell Biol. 2001;21(1):224–34.
22. Kroon E, Krosl J, Thorsteinsdottir U, et al. Hoxa9 transforms primary bone marrow cells through specific collaboration with Meis1a but not Pbx1b. EMBO J. 1998;17(13):3714–25.
23. Golub TR, Slonim DK, Tamayo P, et al. Molecular classification of cancer: class discovery and class prediction by gene expression monitoring. Science. 1999;286:531–7.
24. Andreeff M, Ruvolo V, Gadgil S, et al. HOX expression patterns identify a common signature for favorable AML. Leukemia. 2008;22(11):2041–7.
25. Vezzoli A, Bonadies N, Allen MD, et al. Molecular basis of histone H3K36me3 recognition by the PWWP domain of Brpf1. Nat Struct Mol Biol. 2010;17(5):617–9.
26. Naoe T, Kiyoi H. Gene mutations of acute myeloid leukemia in the genome era. Int J Hematol. 2013;97(2):165–74.
27. Shima Y, Kitabayashi I. Deregulated transcription factors in leukemia. Int J Hematol. 2011;94(2):134–41.

PML mediates glioblastoma resistance to mammalian target of rapamycin (mTOR)-targeted therapies

Akio Iwanami[a], Beatrice Gini[b,c,1], Ciro Zanca[b,1], Tomoo Matsutani[b], Alvaro Assuncao[d], Ali Nael[e], Julie Dang[f], Huijun Yang[b], Shaojun Zhu[g], Jun Kohyama[g], Issay Kitabayashi[h], Webster K. Cavenee[b,i], Timothy F. Cloughesy[j], Frank B. Furnari[b,i,k], Masaya Nakamura[a], Yoshiaki Toyama[a], Hideyuki Okano[l], and Paul S. Mischel[b,i,k,2]

Departments of [a]Orthopaedic Surgery and [l]Physiology, Keio University School of Medicine, Tokyo 160-8582, Japan; [b]Ludwig Institute for Cancer Research, [i]Moores Comprehensive Cancer Center, and [k]Department of Pathology, University of California at San Diego, La Jolla, CA 92093; [c]Department of Neurological, Neuropsychological, Morphological and Movement Sciences, University of Verona, 37134 Verona, Italy; [d]Undergraduate Minor in Biomedical Research Program, and Departments of [g]Molecular and Medical Pharmacology and [j]Neurology, University of California, Los Angeles, CA 90095; [e]Department of Pathology, University of California, Irvine, CA 92697; [f]School of Pharmacy, University of California, San Francisco, CA 94104; and [h]Division of Hematological Malignancy, National Cancer Center Research Institute, Tokyo 104-0045, Japan

Edited[†] by Joseph Schlessinger, Yale University School of Medicine, New Haven, CT, and approved February 1, 2013 (received for review October 12, 2012)

Despite their nearly universal activation of mammalian target of rapamycin (mTOR) signaling, glioblastomas (GBMs) are strikingly resistant to mTOR-targeted therapy. We analyzed GBM cell lines, patient-derived tumor cell cultures, and clinical samples from patients in phase 1 clinical trials, and find that the promyelocytic leukemia (PML) gene mediates resistance to mTOR-targeted therapies. Direct mTOR inhibitors and EGF receptor (EGFR) inhibitors that block downstream mTOR signaling promote nuclear PML expression in GBMs, and genetic overexpression and knockdown approaches demonstrate that PML prevents mTOR and EGFR inhibitor-dependent cell death. Low doses of the PML inhibitor, arsenic trioxide, abrogate PML expression and reverse mTOR kinase inhibitor resistance in vivo, thus markedly inhibiting tumor growth and promoting tumor cell death in mice. These results identify a unique role for PML in mTOR and EGFR inhibitor resistance and provide a strong rationale for a combination therapeutic strategy to overcome it.

mTORC1 | glioma

Glioblastoma (GBM) is the most common malignant primary brain tumor of adults and one of the most lethal forms of cancer (1, 2). As a consequence of frequent EGF receptor (EGFR) amplification and/or activating mutation, other receptor tyrosine kinase amplifications and phosphatase and tensin homolog (PTEN) loss (3, 4), persistent hyperactivation of the phosphatidyl-inositol-3-kinase (PI3K) pathway is observed in nearly 90% of GBMs making the downstream effector, mammalian target of rapamycin (mTOR), a compelling drug target. mTOR links growth factor signaling through PI3K to energy and nutrient status, protein translation, autophagy, and tumor cell metabolism (5). Thus, mTOR is a critical integrator that regulates tumor growth, survival and, potentially, cancer drug resistance.

The allosteric mTOR inhibitor rapamycin has failed in the clinic as a treatment for GBM patients. We previously reported that in a clinical phase I trial for patients with recurrent PTEN-deficient GBM, rapamycin treatment led to Akt activation resulting in loss of negative feedback, consistent with the homeostatic regulatory role of mTOR complex I (mTORC1) as a negative regulator of PI3K/Akt signaling (6). Further, we demonstrated a critical role for mTOR complex II (mTORC2) as a critical mediator of rapamycin resistance through Akt and mTORC1-independent signaling pathways (7). These results have highlighted the potential role for mTOR kinase inhibitors, which block both mTOR signaling complexes, in the treatment of GBM and potentially other cancers.

The interconnectivity between mTOR signaling complexes suggests the possibility that multiple mechanisms of mTOR inhibitor resistance may exist, some of which may be clinically actionable. The promyelocytic leukemia (PML) gene may represent one such mechanism. PML is a pleiotropic tumor suppressor that plays multiple roles on cellular homeostasis such as apoptosis, proliferation, and senescence (8, 9). PML, as part of the retinoic acid receptor (RAR)/PML fusion protein identified in acute promyelocytic leukemia, represents one of the first molecular cancer targets amenable to targeted drug therapy (10, 11). Although the loss of PML protein expression is associated with tumor progression in many tumors (12), some tumors show paradoxically high levels of PML. For example, PML has been shown to be highly expressed in hematopoetic stem cells and in chemotherapy resistant, quiescent leukemia-initiating CML cells (13).

PML is also closely related to receptor tyrosine kinase (RTK)/PI3K/Akt/mTOR signaling pathway at multiple levels. PML has been reported to oppose the function of nuclear Akt (14) and was also identified as a repressor of mTOR through inhibition of Ras homolog enriched in brain (Rheb)–mTOR interaction during hypoxia (15). Further, PML is responsible for the repression of transcriptional activity from the EGFR promoter (16). Considering these factors, we hypothesized that PML might promote resistance to rapamycin, ATP-competitive mTOR kinase inhibitors, and EGFR tyrosine kinase inhibitors by controlling RTK/PI3K/Akt/mTOR signaling and cell cycle in GBM. Here, we examine the expression of PML in GBM cell lines and GBM-patient tissues; show that it is regulated by PI3K/Akt/mTOR signaling; demonstrate the impact of mTOR inhibition on PML expression; and then, using genetic and pharmacological approaches and correlations from clinical samples of patients treated with rapamycin or erlotinib, demonstrate a role for PML in preventing drug-induced apopotosis and promoting clinical resistance. Finally, we identify genetic and pharmacological approaches to overcome this drug resistance.

Results

PML Expression in GBM Patients. To examine the expression of PML in GBM patients, we performed immunohistochemical analysis of GBM by using a tissue microarray (TMA) consisting of multiple representative regions of tumor and adjacent normal tissue from 87 patients with primary GBMs (17, 18). Expression of PML, Ki-67, and phospho-S6 was analyzed and scored independently by two neuropathologists as high or low (scoring summarized in Fig. 1 *A* and *B*). PML was highly expressed in 41.4% of tumor samples (Fig. 1 *A* and *B*), and the expression was

Author contributions: A.I., B.G., C.Z., W.K.C., T.F.C., F.B.F., and P.S.M. designed research; A.I., B.G., C.Z., T.M., A.A., A.N., J.D., H.Y., S.Z., and J.K. performed research; C.Z., T.M., I.K., and F.B.F. contributed new reagents/analytic tools; A.I., B.G., C.Z., T.M., W.K.C., T.F.C., F.B.F., M.N., Y.T., H.O., and P.S.M. analyzed data; and A.I., B.G., C.Z., T.M., W.K.C., T.F.C., F.B.F., M.N., Y.T., H.O., and P.S.M. wrote the paper.

The authors declare no conflict of interest.

[†]This Direct Submission article had a prearranged editor.

Freely available online through the PNAS open access option.

[1]B.G. and C.Z. contributed equally to this work.

[2]To whom correspondence should be addressed. E-mail: pmischel@ucsd.edu.

This article contains supporting information online at www.pnas.org/lookup/suppl/doi:10.1073/pnas.1217602110/-/DCSupplemental.

A

	Ki-67 high	Ki-67 low
PML high	14	22
PML low	45	6

r = -0.5202198, P < 0.01

B

	p-S6 high	p-S6 low
PML high	11	25
PML low	38	13

r = -0.4500150, P < 0.01
(Spearman's rank correlation coefficient)

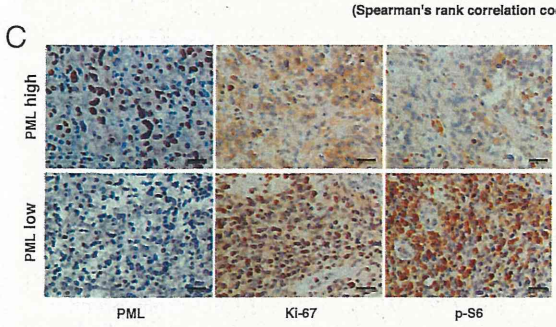

Fig. 1. PML is inversely correlated with proliferation rate and mTOR signaling in GBM clinical samples. (*A* and *B*) Tissue microarrays containing tumor samples from 87 GBM patients were stained by using PML, Ki-67, and p-S6 antibody, respectively. PML is highly expressed in 40% of GBM patients. Correlation analyses show PML significantly inversely correlate with Ki-67 (*A*) and p-S6 (*B*). (*C*) Immunohistochemical staining of (reddish brown) PML, Ki-67, and p-S6 from a representative GBM patient. (Magnification: 10×.) Nuclei were counterstained with hematoxylin (blue). (Scale bar: 100 μm.)

significantly inversely correlated with the cell proliferation marker Ki-67 (Fig. 1 *A* and *C*; $r = -0.52$, $P < 0.01$) and with mTORC1 signaling, as measured by S6 phosphorylation (Fig. 1 *B* and *C*; $r = -0.45$, $P < 0.01$).

Rapamycin Induces Expression and Nuclear Aggregation of PML. Next, we treated GBM cells and a GBM patient-derived cell culture with rapamycin to determine the effect of RTK/PI3K/mTOR inhibitor on PML (Fig. 2 *A*–*C*). Exposure to rapamycin treatment, or the ATP-competitive mTOR kinase inhibitor pp242, at doses sufficient to inhibit mTORC1 signaling, led to time-dependent increases in PML expression (Fig. 2 and Fig. S1). The EGFR tyrosine kinase inhibitor, erlotinib, which inhibited mTORC1 signaling downstream of EGFR, similarly elevated PML expression (Fig. 2*B*). Biochemical results were confirmed by fluorescent immunocytochemical analyses, demonstrating strongly granular patterns of PML staining in the nucleus, consistent with its reported distribution (Fig. 2*C*).

Overexpression of PML Contributes to Decreasing PI3K/Akt/mTOR Signaling and a Slower Cell Cycle. We hypothesized that PML might contribute to rapamycin, mTOR kinase inhibitor, and/or EGFR tyrosine kinase inhibitor resistance in GBM. Therefore, we performed retroviral transduction of PML I into U87 cells and examined the effect on PI3K/Akt/mTOR signaling and cell cycle progression. First, we performed double-immunofluorescent staining with PML and HA tag to confirm the overexpression of PML I (Fig. 3*A*). Compared with control, the retroviral-infected U87 cells expressed exogenous PML in both their nuclei and cytoplasm. Immunoblot analyses of these lysates demonstrated the increased expression of all PML isoforms, which would result from alternative splicing of the longest form, PML I (9). After confirmation of PML overexpression in these cell lines, we examined several PI3K/Akt/mTOR signaling proteins and cell cycle-related proteins by Western blotting. Akt and S6 phosphorylation were significantly decreased in U87 GBM cells that exogenously expressed PML I. Moreover, the cell cycle related proteins, cyclin D1 and cyclin-dependent kinase inhibitor 1 (p21), were also notably decreased, suggesting that PML contributes to decreasing PI3K/Akt/mTOR signaling and slowing down the cell cycle (Fig. 3*B*). We further performed cell proliferation assays by using these cell lines and confirmed that U87PML I cells were significantly less proliferative than control U87 cells (Fig. 3*C*; $^{**}P < 0.01$).

Flow cytometric cell cycle analyses demonstrated an increased G1 fraction in U87PML I-expressing GBM cells (Fig. 3*D*; $^{**}P < 0.01$). To determine whether this conferred rapamycin resistance, we treated U87PML I cells and control cells with rapamycin for 48 h and analyzed the drug effect by using WST-1 assays. PML I overexpression significantly reduced the growth inhibitory effect of rapamycin (Fig. 3*E*; $^{**}P < 0.01$).

Interfering RNA-Mediated PML Knockdown Sensitizes GBM Cell Lines to mTOR and EGFR Kinase Inhibitor Treatment. To confirm a specific role for PML in preventing mTOR and EGFR-kinase inhibitor-dependent cell death, we induced small interfering RNAs (siRNA)-mediated PML knockdown in multiple GBM cell lines and assessed its impact on response to rapamycin, pp242, and erlotinib. TUNEL analysis demonstrated that PML knockdown significantly sensitized all of the GBM cell lines to pp242 and erlotinib-mediated cell death (Fig. 4 *A* and *B*; $^{*}P < 0.05$, $^{**}P < 0.01$), which was confirmed by analysis of polyADP ribose polymerase (PARP) cleavage (Fig. S2). Of note, in contrast to pp242, rapamycin, which has less activity against mTORC2 than does pp242, induced minimal cell death even in the presence of PML knockdown, potentially suggesting a role for sustained mTORC2 signaling in mediating survival (7). Taken together, these data demonstrate that PML contributes to mTOR and EGFR kinase inhibitor resistance in GBM by suppressing tumor cell death, which can be reversed by pharmacological or genetic inhibition of PML.

As_2O_3 Abrogates pp242-Induced PML Up-Regulation and Sensitizes GBMs to mTOR Kinase Inhibitor-Mediated Cell Death. Arsenic trioxide (As_2O_3) has long been used as a therapeutic agent for promyelocytic leukemia (19–21). Besides its cell toxicity, As_2O_3 has been shown to target PML for degradation through a sumoylation-dependent process leading to PML polyubiquitination and proteosomal degradation (11, 13, 22–24). Therefore, we investigated the effect of As_2O_3 on reduction of PML in U87 cells. Single As_2O_3 treatments reduced PML expression at both low (0.15 μM) and high concentrations (2 μM) and decreased proliferation in serum-containing growth condition (Fig. S3 *A* and *B*). Notably, a high concentration (2 μM) induced an increase in p53 levels and decreased levels of cyclin D1 expression (Fig. S3*A*). The ability of low dose As_2O_3 to inhibit proliferation in the absence of p53 induction is consistent with previous papers (13, 25)

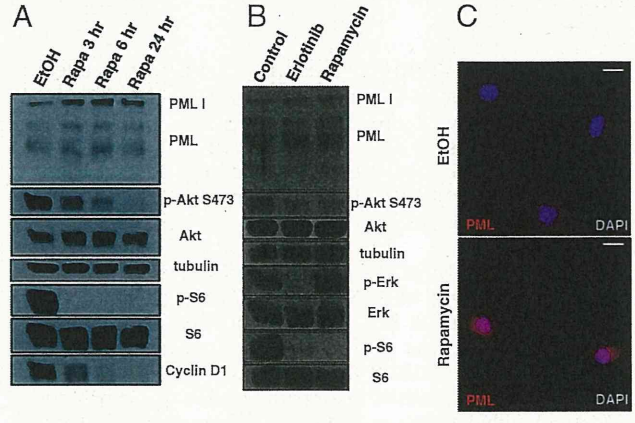

Fig. 2. PI3K/Akt/mTOR inhibitors induce PML expression in GBM cells. (*A*) Western blot analysis of the effect of rapamycin treatment on PML expression in U87 cells. Cells are cultured in serum-free condition. (*B*) Effect of the EGFR inhibitor erlotinib and rapamycin on PML expression in GBM patient-derived cells. Cells are cultured under neurosphere conditions. (*C*) Immunofluorescence of PML (red) in U87 cells treated with rapamycin or control. Nuclei are stained with DAPI (blue). (Scale bar: 20 μm.)

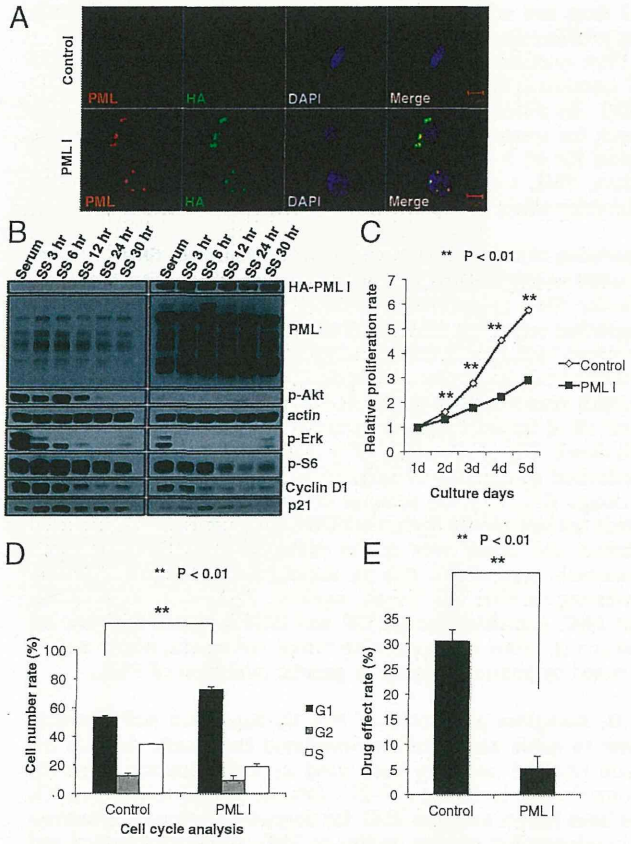

Fig. 3. PML overexpression decreases PI3K/Akt/mTOR signaling and slows down cell cycle. (*A*) Immunofluorescence in U87 control or hemagglutanin-tagged PML1 (HA-PMLI) infected cells. (Scale bar: 10 μm.) (*B*) Western blot analysis of PI3K/Akt/mTOR signaling pathway and cell cycle-related proteins performed on lysates from U87 control or HA-PMLI infected cells. Cells were placed in serum-free medium, cultured, and collected in each time course. (*C*) Proliferation of U87 control and HA-PMLI infected cells analyzed by WST assay. *P* value was determined by Student's *t* test. (*D*) Effect of PMLI overexpression on cell cycle progression in U87 cells. Cell cycle distribution was performed by flow cytometric analysis. *P* value was determined by Student's *t* test. (*E*) Effect of treatment with rapamycin on growth of U87 control and HA-PMLI infected cells analyzed by WST assay. *P* value was determined by Student's *t* test.

suggesting that lower concentration of As_2O_3 mediates its effect by reducing PML levels and not by inducing DNA damage. Neither pp242, nor As_2O_3 alone, promoted extensive tumor cell death. In contrast, As_2O_3 (0.15 μM) significantly and synergistically promoted pp242- dependent apoptotic cell death, as measured by cleaved caspase and TUNEL staining, independent of any effect on p53 phosphorylation (*$P < 0.01$; Fig. 5 *A* and *B* and Fig. S3*C*).

Therefore, we analyzed the effect of combining the mTOR kinase inhibitor pp242 with As_2O_3 on PML expression, cell death, and tumor size in U87 GBM xenografts (Fig. 5 *C–F*). Sixteen days of treatment with pp242 and As_2O_3, significantly reduced the growth of GBMs by nearly threefold ($P < 0.0005$) and induced TUNEL-positive cell death, an effect that was not detected with either pp242 or As_2O_3 monotherapy (Fig. 5 *C*, *D*, and *F*). Importantly, As_2O_3 also abrogated the pp242-mediated up-regulation of PML expression (Fig. 5*E*). Ki-67 staining was also diminished, although the decrease failed to reach statistical significance (Fig. S4). Taken together, these results demonstrate that As_2O_3 dramatically synergizes with mTOR kinase inhibition to promote GBM cell death and block tumor growth in vivo.

Immunohistochemical Analyses of PML Expression in GBM Patients Treated with Rapamycin or Erlotinib. Finally, to establish clinical relevance and to determine whether PML up-regulation is associated with mTOR and EGFR inhibitor resistance in GBM patients, we performed immunohistochemical analyses of tumor samples obtained from two "biopsy-treat-biopsy" paradigm phase I clinical trials, for which tumor tissue was obtained 7–10 d after treatment with rapamycin or lapatinib (details presented in refs. 6 and 26). As shown in Fig. 6, rapamycin (Fig. 6 *A* and *B*) and erlotinib (Fig. 6 *C* and *D*) treatment were both associated with significantly enhanced nuclear PML expression (*$P < 0.01$).

Discussion

PML is a pleiotropic tumor suppressor protein that is lost in many cancer types (12, 27). PML negatively regulates Akt-mTOR signaling (14, 28) and suppresses PTEN loss- induced prostate tumorigenesis (14) and mTOR-dependent renal carcinoma progression (28). We provide evidence from preclinical models and in patients that PML suppresses Akt/mTOR signaling and proliferation (Fig. 1). However, PML is also commonly overexpressed in cancer, including in GBM (12, 29), and has been shown to promote a range of activities that may enhance the growth and progression of cancer, including oncogene-induced senescence (29), hematopoetic stem cell maintenance, and breast cancer tumor cell survival through a peroxisome

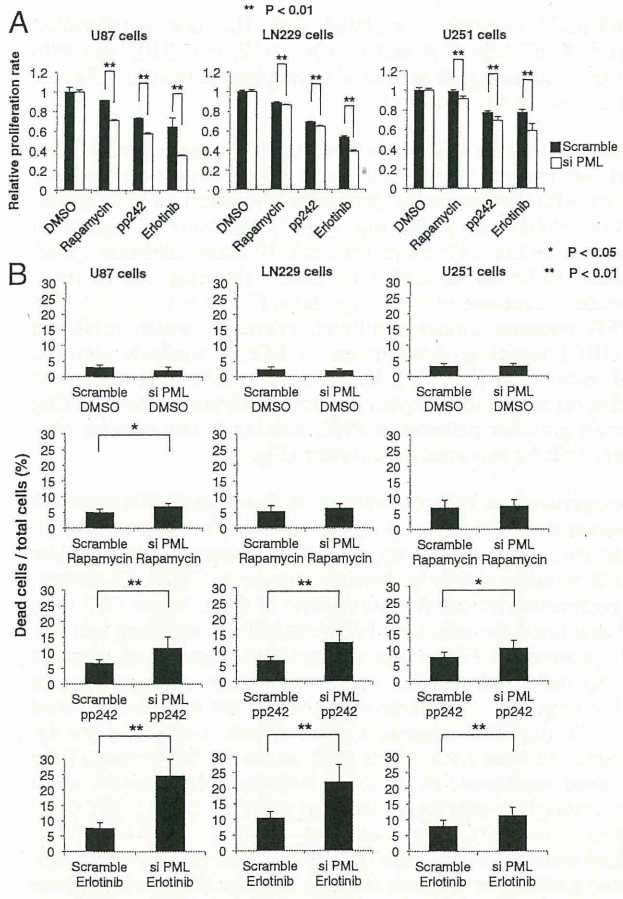

Fig. 4. PML knockdown sensitizes GBM cell lines to EGFR and mTOR targeted therapies. (*A*) Cell viability assays demonstrate a synergistic effect of PML knockdown and each indicated inhibitor. *P* values were determined by Student's *t* test. (*B*) Effect of PML knockdown and each indicated inhibitor on multiple GBM cell lines analyzed by Trypan blue exclusion. *P* values were determined by Student's *t* test.

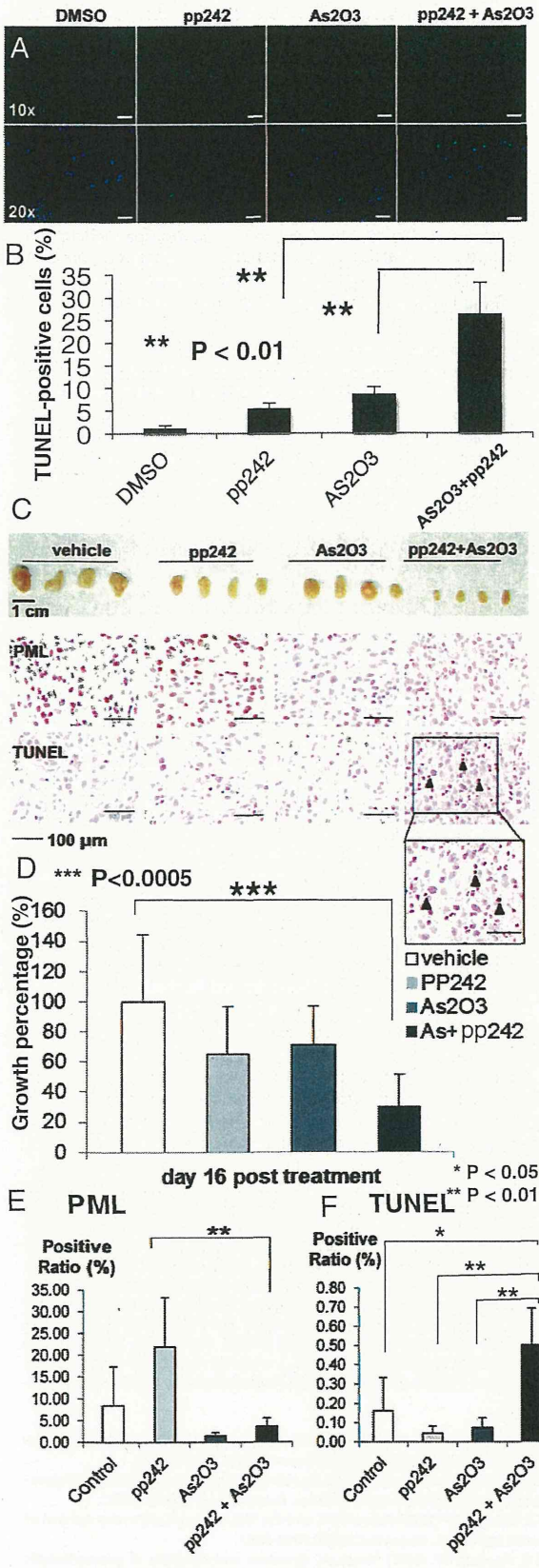

Fig. 5. As_2O_3 reduces PML and sensitizes GBM cells to mTOR-targeted therapies. (*A*) Representative images demonstrating TUNEL staining (green) to assess apoptotic effect of pp242 and As_2O_3 (2 μM) on U87 cells in vitro. Nuclei are stained blue. (*B*) Quantification of TUNEL staining. *P* values were determined by Student's *t* test. (*C*) Representative photographs of U87 GBM xenografts treated daily with vehicle, pp242 (60 mg/kg per day by oral gavage), As_2O_3 (2.5 mg/kg intraperitoneally), or combination ($n = 8$ mice per condition). Images of representative PML and TUNEL stains. (*D*) Quantification demonstrating greater than threefold reduction in tumor size for mice treated with combined pp242 and As_2O_3 ($P < 0.005$). (*E* and *F*) Quantification of PML and TUNEL xenograft tumor staining from each treatment conditions.

proliferator-activated receptor (PPAR)-γ/fatty acid oxidation-dependent pathway (30, 31). Further, PML has been shown to mediate resistance of leukemias to chemotherapy by supporting maintenance of a "quiescent" tumor cell population (13). Its impact on cancer drug resistance, including drugs that target mTOR or its upstream effectors, in solid tumors including GBM is less clear. Through integration of preclinical studies with analysis of tumor tissue from patients in phase I clinical trials, we demonstrate an important role for PML in mediating mTOR and EGFR inhibitor resistance in GBM. These results present evidence that mTOR inhibition promotes PML up-regulation in patients and that this up-regulation of PML mediates drug resistance.

It is tempting to speculate that PML promotes this resistance by inducing a "quiescent state" through inhibition of Akt/mTOR signaling. However, we cannot formally exclude the possibility that PML may drive resistance through its metabolic prosurvival effects. In fact, this possibility is consistent with our previous observation that EGFR mutant GBMs have enhanced reliance on fatty acid synthesis for survival (17), creating enhanced dependence on fatty acid oxidation for survival (32). Futures studies will be needed to determine the mechanisms by which PML promotes drug resistance in GBM.

mTOR has emerged as a critical target in GBM because it is persistently hyperactivated downstream of the most common GBM alterations including EGFR amplification, EGFR variant III (EGFRvIII) mutation, platelet-derived growth factor receptor (PDGFRα) and hepatocyte growth factor receptor (c-MET) amplification, and PTEN loss (3). We have demonstrated that mTOR inhibition is required for the efficacy of EGFR-targeted therapies (33), suggesting a mechanistic basis by which EGFR tyrosine kinase inhibitors (TKIs) may also potently up-regulate PML expression to promote drug resistance. For both EGFR TKIs and mTOR kinase inhibitors, the potential for converting a cytostatic response, which often yields minimal benefit, to a cytotoxic response by pharmacologically abrogating PML, could potentially represent a significant clinical advance. Our demonstration of a synergism between the two classes of compound in cell death induction underscores this possibility.

Pharmacologically targeting PML represents one of the most exciting success stories for the principle of molecularly guided therapies (10, 11). As_2O_3 targets PML for degradation through a SUMOylation-dependent process (34), potently promoting long-term remission in patients and mice with acute promyelocytic leukemia bearing the PML/RAR fusion (24). Its role in solid cancers has yet to be established. However, As_2O_3 given with standard chemotherapy can be tolerated by GBM patients, as demonstrated in recent clinical trials (35). The results presented here suggest a clinically actionable strategy to combine resistance by combining As_2O_3 with mTOR kinase and EGFR TKIs for the treatment of GBM patients.

Materials and Methods

Cell Lines. U87, LN229, and U251 GBM cell lines were cultured as previously described (18, 26). Brain tumor samples were collected after surgical resection under University of California, Los Angeles (UCLA) institutional review board-approved protocols between 1999 and 2011 from patients who gave informed consent, and graded by the neuropathologist in accordance with World Health Organization-established guidelines. Neurosphere cultures were prepared as described (36). Full details are provided in *SI Materials and Methods*.

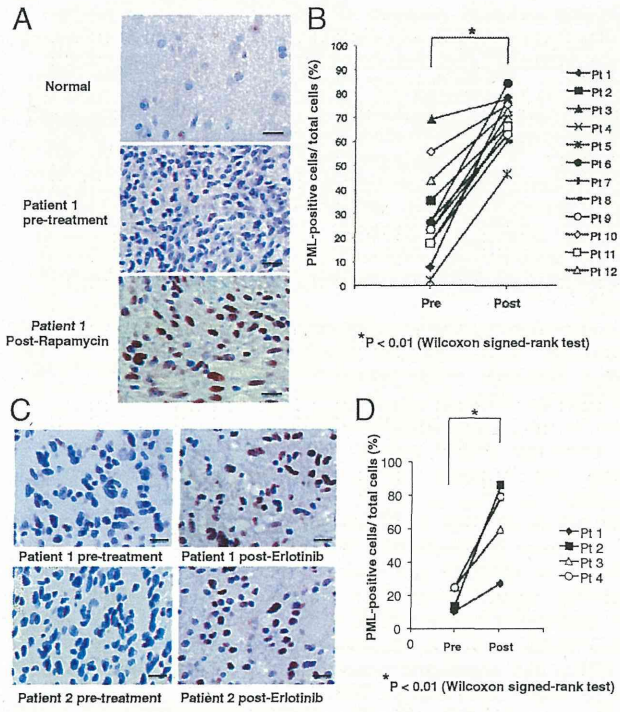

Fig. 6. Rapamycin and erlotinib treatment induces PML expression in GBM patient tumor tissues. (*A*) Immunohistochemical staining (reddish brown) of PML before and after treatment with rapamycin. Nuclei were counterstained with hematoxylin (blue). (*B*) Quantification of immunohistochemical staining from >1,000 cells from at least three representative areas of each tumor before and after rapamycin treatment. *P* value was determined by Wilcoxon signed-rank test. (*C*) Immunohistochemical staining (reddish brown) of PML before and after treatment with erlotinib. Nuclei were counterstained with hematoxylin (blue). (*D*) Quantification of immunohistochemical staining from >1,000 cells from at least three representative areas of each tumor before and after erlotinib treatment. *P* value was determined by Wilcoxon signed-rank test. (Scale bars: 50 μm.) (Magnification: 20×.)

Antibodies and Reagents. We used antibodies directed against the following: phosopho-Akt Ser473, Akt, phospho-S6 Ser235/236, S6, phospho-Erk, Erk, CyclinD1, cleaved PARP (Cell Signaling); β-actin, p21 (Sigma); phospho-EGFR Tyr1086 (Invitrogen); EGFR (Millipore); PML (for Western blotting, Abcam; for immunohistochemisry, Santa Cruz). Reagents used are rapamycin, As_2O_3, polybrene (Sigma), erlotinib (ChemieTex), pp242 (Chemdea). Full details of immunoblot analysis are provided in ***SI Materials and Methods***. Stock solutions of inhibitor for rapamycin were made by dissolving in ethanol, erlotinib, and pp242 were made by dissolving in DMSO (Sigma) and stored at −20 °C. Inhibitors were added to each well at final concentrations of 10 nM, 10 μM, and 2 μM, respectively. An equal concentration of ethanol or DMSO served as control. As_2O_3 was diluted by PBS and 10 M NaOH, then pH was adjusted at 8.0 by 12 M HCl.

Plasmid, Retroviral Infection, and siRNA Transfection. Plasmid 22(pLNCX) encoding hemagglutinin (HA) tag-expression construct was obtained from the I.K. laboratory (37). Full details are available in ***SI Materials and Methods***. Transfection of siRNA into GBM cell lines was carried out by using Lipofectamine RNAiMAX (Invitrogen) in full serum, with medium change after 24 h. On-TARGET plus SMARTpool siRNAs (Dharmacon) specifically targeting PML (catalog no. L-006547-000005) and nontargeting control pools of siRNAs (catalog no. D-0018-10-10-05) were used at 10 nM, and cells were harvested 48 h after transfection.

Cell Proliferation and Death Assays. Relative proliferation to control cells with vehicle treatment was checked with a WST-1 Cell Proliferation Assay Kit (Millipore). Cell death was assessed by Trypan blue exclusion (Invitrogen). Full details are given in ***SI Materials and Methods***.

Cell Cycle Analyses. Cells were fixed in 70% ethanol diluted in PBS, and the samples were stored at −20 °C. The fixed cells were resuspended in PBS containing 20 μg/mL propidium iodide (Sigma) and 10 μg/mL RNase A (Sigma), and incubated for 10 min at 37 °C. Flow cytometric analysis was performed by using FACSCalibur flow cytometer (Becton Dickinson).

TUNEL Staining and Immunofluorescence Analysis. For TUNEL staining, cells were placed in eight-well chamber slides, incubated with TUNEL Reaction Mixture (Roche) at 37 °C for1 h in the dark, and visualized with a fluorescene microscope (Olympus BX-61). Ten separate, randomly chosen fields on each chamber were imaged, and the numbers of TUNEL-positive cells and whole nuclei were counted. For immunofluorescence analysis with indicated antibodies, cells were fixed with 4% paraformaldehyde in PBS for 10 min, washed twice in PBS, incubated with primary antibodies in PBS containing 3% BSA at 4 °C overnight, and detected with appropriate fluorescence-conjugated secondary antibodies. Full details are presented in ***SI Materials and Methods***.

In Vivo Studies. We suspend 1.25×10^6 U87 GBM cells in 100 μL of Matrigel, PBS 1:2 solution, and injected them subcutaneously into the right flank of each 4- to 5-wk-old athymic nude mice. Tumors were measured with an electronic caliper, and volumes were calculated by using width (*a*), length (*b*), and depth (*c*) measurements ($V = a \times b \times c$). Ten days after injection, mice were treated daily with vehicle, 60 mg/kg pp242 by gavage, 2.5 mg/kg intraperitoneally injected As_2O_3 or their combination, respectively. Mice were euthanized when tumor volume of treated mice reached statistical significance compared with control groups. Mice were euthanized in accordance with the University of California at San Diego Institutional Guidelines for Animal Welfare and Experimental Conduct.

Immunohistochemical Assays, Tissue Microarrays, and Image Analysis-Based Scoring. Immunohistochemical staining and analysis of two GBM TMAs was performed, as described (6, 26). Among 140 cases, 87 GBM patient tissue cores were available for analysis based on sufficient high quality tissue. Staining intensity was scored independently by two pathologists who were unaware of the findings of the molecular analyses. See ***SI Materials and Methods*** for full details.

Statistical Analysis. Results are shown as mean ± SEM. χ^2 for independence test was used to assess correlations between various molecular markers on TMAs. For nonparametric clinical trial data, Wilcoxon rank test was used. Other comparisons in cell proliferation assays, cell death assays, and TUNEL staining were performed with Student's *t* test, as by analysis of variance, appropriate. $P < 0.05$ was considered as statistically significant.

ACKNOWLEDGMENTS. We thank Dr. George Thomas for helpful discussions and comments on this paper. A.I. and J.K. were supported in part by a grant from the Japan Society for the Promotion of Science. A.I. was also supported by a grant from the Uehara Memorial Foundation. B.G. is supported by a Marie Curie Fellowship from the European Commission- PIOF-GA-2010-271819. C.Z. is supported by an American-Italian Cancer Foundation post-doctoral research fellowship. This work was supported by National Institutes of Health (NIH) Grants NS73831 and CA119347 (to P.S.M.), by the Ziering Famiy Foundation in memory of Sigi Zeiring (P.S.M. and T.F.C.), the Ben and Catherine Ivy Foundation (P.S.M. and T.F.C.), and NIH Grant P01-CA95616 (to W.K.C.). W.K.C. is a Fellow of the National Foundation for Cancer Research.

1. Furnari FB, et al. (2007) Malignant astrocytic glioma: Genetics, biology, and paths to treatment. *Genes Dev* 21(21):2683–2710.
2. Wen PY, Kesari S (2008) Malignant gliomas in adults. *N Engl J Med* 359(5):492–507.
3. Anonymous; Cancer Genome Atlas Research Network (2008) Comprehensive genomic characterization defines human glioblastoma genes and core pathways. *Nature* 455(7216):1061–1068.
4. Parsons DW, et al. (2008) An integrated genomic analysis of human glioblastoma multiforme. *Science* 321(5897):1807–1812.
5. Yecies JL, Manning BD (2011) Transcriptional control of cellular metabolism by mTOR signaling. *Cancer Res* 71(8):2815–2820.
6. Cloughesy TF, et al. (2008) Antitumor activity of rapamycin in a Phase I trial for patients with recurrent PTEN-deficient glioblastoma. *PLoS Med* 5(1):e8.
7. Tanaka K, et al. (2011) Oncogenic EGFR signaling activates an mTORC2-NF-κB pathway that promotes chemotherapy resistance. *Cancer Discov* 1(6):524–538.
8. Bernardi R, Pandolfi PP (2003) Role of PML and the PML-nuclear body in the control of programmed cell death. *Oncogene* 22(56):9048–9057.
9. Bernardi R, Pandolfi PP (2007) Structure, dynamics and functions of promyelocytic leukaemia nuclear bodies. *Nat Rev Mol Cell Biol* 8(12):1006–1016.
10. Andre C, et al. (1996) The PML and PML/RARalpha domains: From autoimmunity to molecular oncology and from retinoic acid to arsenic. *Exp Cell Res* 229(2):253–260.